JP1.1 REAL-TIME MULTI-SATELLITE PRECIPITATION ESTIMATION AND ASSIMILATION

Mohan Nirala* and Paul Houser
NASA Goddard Space Flight Center, Greenbelt, Maryland

1. INTRODUCTION

Rain measurements from rain gauges have been used from centuries globally covering only land areas. The satellite observation was recognized after the first launch of Defense and Meteorological satellite program (DMSP) satellite in 1987, equipped with multi frequency passive microwave radiometer Special Sensor Microwave Imager (SSM/I). The SSM/I gave better precipitation data globally over both land and ocean regularly. It is recognized that satellite-based data are a foremost tool for measuring precipitation. NASA initiated a new research program to measure precipitation from space under its Mission to Planet Earth program in the 1990s (Smith et al. 1994, 1998, Nirala and Cracknell 2002 a, b). As a result, the Tropical Rainfall Measuring Mission (TRMM), a collaborative mission between NASA and NASDA, was launched in 1997 to measure tropical and subtropical rain (Simpson et al. 1996 and Kummerow et al. 2000). Motivated by better results as compared to SSM/I and the success of TRMM, and recognizing the need for more comprehensive global precipitation measurements, NASA and NASDA have now planned a new mission, the Global Precipitation Measurement (GPM) mission (Shepherd et al. 2002). The primary goal of GPM is to extend TRMM's rainfall time series while making substantial improvements in precipitation observations, specifically in terms of measurement accuracy, sampling frequency, Earth coverage, and spatial resolution.

GPM will acquire global precipitation data sufficient to resolve the diurnal cycle using a core spacecraft operating in a 65° inclination orbit and a constellation of dedicated and existing spacecraft operating in various orbits, mostly Sun-synchronous, spaced approximately three hours apart (Shepherd et al 2002). The spacecraft will be supported by an array of ground validation and calibration sites that provides ground-based observations of rain and clouds at specific geographic locations. The mission consists of a Dual-frequency Precipitation Radar (DPR) and the GPM Microwave Imager (GMI), and a constellation of precipitation-measuring spacecraft. The GPM core spacecraft is planned to launch in fiscal year 2008 with - operational orbit at 65° inclination and 400 km circular orbit. One NASA constellation spacecraft is also planned for launch in the same timeframe to a sun-synchronous orbit of 635 km. DMSP satellites will continue to fill two constellation slots. The objectives of GPM are: (1) to provide improved climate observations and prediction, (2) to improve the accuracy of precipitation forecasts and weather prediction, and (3) to provide improved understanding of the global water cycle, including flood and fresh water resources prediction. The GMI will have, as a minimum, the same capabilities as the TMI. As a result of its constellation operation GPM will provide diurnally-resolved, near global coverage of precipitation at surface resolution of 10 km. In order to make rainfall measurements on a global basis every three hours, up to eight satellite will be required.

The TRMM TMI data is currently available and used in precipitation measurements. The spatial resolution of the TMI ranges from 5 km at 85.5 GHz to 45 km at 10.65 GHz. The TMI operates on 5 frequencies of 10.65, 19.35, 22.235, 37.0 and 85.5 GHz. The TMI is similar to the Special Sensor Microwave Imager (SSM/I) instrument flown on the Defense Meteorological Satellite Program (DMSP). TRMM mission provides daily precipitation estimate between 40° N to 40° S longitude that can be used for the Global Land-surface Data Assimilation System (GLDAS). The DMSP SSM/I data can be used to get precipitation beyond the tropics. Data assimilation merges a range of diverse data fields with model prediction to provide the model with the best estimate of the current state of the natural environment so can then make more accurate prediction. Data assimilation offers an attractive way to merge and interpret hydrological information provided by satellite and ground- based observations.

The goal of this paper is to study of the space-borne retrieved rainfall and related products using GLDAS. The main aims of this investigation are diagnosis to ascertain the causes of errors with satellite precipitation products, improvement of satellite precipitation products and evaluation to estimate the quality of satellite precipitation products in terms of systematic and random error and comparison of various satellite derived rain product with ground data. This research will place emphasis on merging different satellite observations of precipitation to develop a high resolution spatial coverage, hourly temporal coverage precipitation product using TMI, SSM/I data. Observation, corrections and elimination of error in

*Corresponding author address: Mohan L. Nirala, Hydrological Sciences Branch, code 974, NASA Goddard Space Flight Center, Greenbelt, MD 20771. email:mnirala@hsb.gsfc.nasa.gov

precipitation estimation will be carried out using findings from several projects such as Global Precipitation Climatology Project (GPCP), Global Precipitation Measurement (GPM) and International satellite Cloud Climatology Project (ISCCP) etc. The emphasis of this research will be also on assimilation of remotely sensed observations of precipitation using TMI, SSM/I, with UCAR Community Land Model and development of assimilation methods making best use of all available data and information, identification of errors and accuracy of the data assimilation products. This research is still in the preliminary stage to utilize and improve the existing real-time multi-satellite precipitation estimation in the hydrological models and compare the results with several other precipitation product and observations.

2. MULTI-SATELLITE PRECIPITATION

The techniques to enable the high temporal and spatial resolution combined precipitation data can facilitate the use of hydrological model to determine the impact of precipitation uncertainties on the model output. This research is in the preliminary stage in this direction to determine the precipitation uncertainties. High-quality estimates of the amount, temporal evolution, and spatial distribution of precipitation are important for a wide range of scientific and applications-related research such as weather forecasting, flood prediction and control, water resources prediction, hurricane monitoring. Although, measurement of less dynamic and more homogenous meteorological fields such as pressure or even temperature, accurate measurement of precipitation is particularly challenging due to its highly stochastic and rapidly changing nature. It is quite common to observe a wide range of precipitation rates within a given time frame at a given location. Significant research has been done to improve the temporal and spatial resolution of precipitation estimation. Furthermore, precipitating systems generally exhibit non-homogeneous spatial distributions of rain rates over local to regional domains. High temporal and spatial sampling of precipitation is preferred in many research and applications problems. Over land, rain gauges and radars are often appropriate for this purpose but generally lack sufficient coverage in particular area. Ground-based radar suffers from instrument error, calibration error, topographic blocking, beam broadening, beam overshoot, and non-unique reflectivity rain rate relationships. More than two-thirds of the Earth is covered with ocean. This suggests that satellite estimation is the only mean to get global coverage. Several Microwave radiometers and rain radars flown on low altitude satellites have offered the more accurate retrievals, although they are limited by the intrinsic sampling capabilities intrinsic to low-earth orbits. Morrissey and Janowiak (1996) found that pentad and monthly estimates of rainfall introduces temporal sub-sampling uncertainties that introduce conditional bias, which can cause over-estimation or under-estimation of precipitation depending upon the ambient precipitation rate. For a 3-hourly sampling scheme, the bias is close to zero but increases markedly for a 12-hour sampling scheme. Li et al. (1996) demonstrated that the start-up time of a sampling scheme is as important as the sampling scheme itself, due to bias introduced by the diurnal cycle of precipitation. For arbitrary start-up times, they found a minimal bias for a 3-hourly sampling scheme relative to a 12-hourly scheme. Soman et al. (1995) found similar results using Darwin radar data. In light of these findings and others, 3-hourly sampling is a reasonable and actually an attainable goal with today's and the near future's mix of satellite assets. Combined precipitation estimation is used to derive long term precipitation statistics and utilization as an input in hydrological models.

There are several rainfall data products in varieties of data processing and analyzing techniques. Adler et al. (2000) are currently using a combination of TRMM and geosynchronous Infrared IR (geo-IR) data to provide 3-hourly estimates of precipitation over 50°N-50°S using an approach based on TRMM real-time multi-satellite algorithm 3B42. This product initially uses a combination of TRMM estimates and TRMM calibrated SSM/I estimates. Significant Improvement has been done in the passive microwave algorithm development. However, because of the low Earth orbit sampling properties of TRMM and DMSP satellites leave spatial gaps at the 3-hour time resolution, microwave-calibrated geo-IR estimates are used to fill the gaps (Shepherd et al 2002). Clearly, the evolving era of merged multiple satellite rain estimates underpinned by a reliable calibrating source such as TRMM represents a valuable testbed for developing the GPM constellation mission's data processing system. Moreover, there are genuine scientific concerns with the current techniques used to estimate precipitation from geo-IR data streams in order to achieve high temporal resolution (Shepherd et al 2002).

The precipitation estimates are available from several satellites and ground observations which their own sources of strengths and weaknesses. The geostationary observations provide better temporal resolution and diurnal coverage of the precipitation systems. The current TRMM approach to achieve high temporal precipitation sampling, i.e., to estimate 3-hourly rainfall maps, employs geo-IR measurements to fill temporal gaps not sampled by the TRMM satellite. While the robust temporal coverage provided by geosynchronous infrared data has been an unchallenged asset of the world's geostationary satellite network, geo-IR retrieval algorithms have been problematic since the first attempts to use them began in the mid 1970s. However, the accuracy of the IR data

rain estimate is not that good as compared to the microwave rain measurements. The major shortcoming is that they suffer from underlying weak statistical relationships between IR radiances at cloud top (generally represented as equivalent black body temperatures or (EBBTs)) and rainfall at the surface (Shepherd et al. 2002). In the recent reviews of Bellerby et al. (2000) and Ba and Gruber (2001) concerning several well-established geo-IR techniques used in the operational community, these problems are underscored. The IR rain estimation techniques are based on cloud top temperature, brightness etc. The standard assumption behind IR techniques is that cold cloud tops (e.g., cloud EBBTs below some threshold) are directly associated with precipitating cumulonimbus clouds. The geo-IR techniques largely perform as convective precipitation algorithms and several attempts have been made with marginal success to classify cold clouds into convective or stratiform categories according to EBBT texture signatures (Shepherd et al 2002). However, high-level cirrus and other non-precipitating clouds often exhibit cloud-top temperatures below the screening threshold, which can create false precipitation estimates. This results in inherent overestimation of rainfall when cirrus and other cold cloud tops are present. The relationship between infrared radiance and surface precipitation is very weak but it may be better and useful in the deep convection systems in tropics. If the estimates are later bias-adjusted according to a microwave algorithm, the procedure which the TRMM algorithm incorporates, the average rain rates applied to the true raining areas must be underestimated to compensate for assigning positive rain rates to the false areas. Geo-IR techniques are also generally found to underestimate rainfall from stratocumulus clouds, which are ubiquitous in mid-latitude coastal regions, because much of the drizzle regions of the stratocumulus decks have cloud top temperatures warmer than the precipitation cutoff (shepherd et al 2002). In the case of altostratus and multi-layered cloud systems, geo-IR-techniques exhibit variable performance according to the ambient thermal conditions. Further difficulties are introduced by the inability of these techniques to sense any direct information on rainfall occurring below the cloud bases of precipitating clouds as Bellerby et al. (2000) has discussed. In addition, geo-IR techniques must apply significant downscale averaging to achieve any meaningful accuracy. For these reasons and other more subtle problems, 3-hourly estimates using geo-IR calibration and merging techniques are susceptible to significant uncertainties. Microwave measurements are used to adjust the IR based techniques. In general, Infrared techniques possess bias and precision uncertainties for 3-hour estimates exceeding 20% and 50%, respectively, with little room to improve because there are no meaningful physics tools to exploit in making the estimates (Shepherd et al. 2002). Currently several rain estimation methods use IR techniques to get better temporal coverage despite the drawbacks in accuracy assessment as compared to Microwave techniques.

Measurement of precipitation in global scale with better resolution is long-term objectives of the several research communities. It is the GPM, which represents the next generation of space-based precipitation estimation and builds upon valuable techniques with knowledge and experience gained during the TRMM mission. In the GPM era, up to nine constellation satellites will provide more accurate and physically-based microwave precipitation estimates on a global basis with ~5% bias and ~20% precision uncertainty for 3-hourly products (Shepherd et al. 2002). Such direct measurements of precipitation and hydrometeor structure mitigate errors introduced by non-precipitating clouds, diverse macro cloud physics, and varying precipitation types. It is very useful for data assimilation research and several other scientific issues to have better global precipitation and not only in the tropics. GPM's Dual Frequency Precipitation Radar (DPR) and up to nine passive microwave radiometers (PMRs) on the constellation satellite of GPM will provide an excellent means to cross-calibrate similar precipitation-measuring instruments in space and on the ground validation sites. Thus, GPM will enable improved measurements of light rain, warm rain, snow, and other modes of frozen precipitation. The DPR will better detect explicit precipitation microphysics than was possible from the single frequency TRMM Precipitation Radar (PR), thereby leading to improvements in latent heating algorithms and mass spectra properties associated with the highly varying drop size distribution (DSD). GPM satellites will be used for weather forecasting and environmental research with microwave radiometers able to provide better precipitation measurements. GPM is also important because from an end-user perspective it will almost seamlessly advance a rainfall product line from the TRMM era in which acquiring the first complete and accurate tropical climatology of rainfall was the major objective, to an era where high frequency sampling, complete global coverage, microphysical variability, and thorough error quantification will become a reality (Shepherd et al. 2002). All of these new capabilities are needed for a significant improvement in our understanding of the global water and energy cycle and in detecting actual accelerations or decelerations in the water cycle that are associated with changes in the Earth's climate system, particularly in terms of global temperatures. While TRMM provides the rain data, the GPM will extend the future comprehensive with near-global coverage precipitation and improve observation of light rain in high latitudes.

3. ALGORITHMS AND DATA ANALYSIS

The TMI and SSM/I data will be used in the algorithm as an input to the model (i.e. CLM), which are describe in more detail in the next section. The Goddard Profiling Algorithm (GPROF) is based on Kummerow et al. (1996) and Olson et al. (1999). GPROF is a multi-channel physical approach for estimating rainfall and vertical structure of rainfall microphysics from satellite-based passive microwave observations (such as SSM/I and TMI). The GPROF-SSM/I estimates are computed from the SSM/I SDRs as part of the RT Data Set, while the GPROF-TMI estimates are computed by TSDIS as 2A12RT. The current version (denoted as "5" in TRMM) applies a Bayesian inversion method to the observed microwave brightness temperatures using an extensive library of cloud-model-based relations between hydrometeor profiles and microwave brightness temperatures (Huffman et al 2002). Each hydrometeor profile is associated with a surface precipitation rate. GPROF includes a procedure that accounts for inhomogeneities of the rainfall within the satellite instantaneous field of view (IFOV). Over land and coastal surface areas the algorithm reduces to a scattering-type procedure using only the higher-frequency channels such as 37 and 85.5 GHz. This loss of information arises from the physics of the emission signal in the lower frequencies when the underlying surface is land or other than all water. This algorithm is applied to both the TMI and SSM/I data and the estimates are used as input to RT Data Set processing. Satellite Data Records (SDR) containing level 2 (scan-pixel) SSM/I brightness temperature (T_b) data are provided by the Department of the Navy, Fleet Numerical Meteorological and Oceanographic Center, Monterey, CA (Turk et al 2000). Each file contains a "contact" of down-linked data, which can be up to 2 orbits. The data have had some quality control, and are converted from sensor units to antenna temperature T_a, then to T_b, as well as providing numerous other physical quantities and metadata (Huffman et al 2002). These data are used as input to GPROF-SSM/I for use in RT Data Set processing. TSDIS algorithm 2A12RT contains level 2 (scan-pixel) GPROF estimates of precipitation based on TMI data. These are provided by TSDIS. Each file contains an orbit of estimates. These data are used as input to RT Data Set processing. The TMI data provided by TSDIS will be also used as input in the NCAR Community Land Model (CLM) to assimilate the precipitation data product.

Combined microwave (TMI, SSM/I) High Quality (HQ) precipitation measurement provides a global 0.25°x0.25° averaged 3-hourly combination of all available SSM/I and TMI estimates (Huffman et al. 2002). The GPROF-SSM/I is probability-matched to 2A12RT. The GPROF-SSM/I and 2A12RT estimates are gridded to a 0.25°x0.25° global grid for a 3-hour period centered on the major synoptic times (00Z, 03Z, 06Z, 09Z, 12Z, 15Z, 18Z, 21Z) and the GPROF-SSM/I estimates are calibrated to 2A12RT. The rain rate produced in each grid box is the pixel-weighted average of all grid boxes contributing during the 3 hours. Additional fields in the data file include the number of pixels, the number of pixels with non-zero rain, and the number of pixels for which the estimate is "ambiguous," or highly uncertain. The SSM/I data are available in the latitude band 85° N-S, but GPROF-SSM/I only returns estimates in the band 70° N-S. Additionally, GPROF-SSM/I is unable to provide estimates in regions with frozen or icy surfaces.

The brightness temperature data in high frequencies are subjected to a discrimination process and each pixels are tested for presence of rain and no rain. These data are processed using the algorithm and an output 3B40RT is generated. The units of the Real Time data set estimates are mm/hour for the precipitation and random error estimates, dimensionless for the source field, and number of pixels for the other fields. The global grid on which each precipitation values are presented is 0.25°x-.25° (Cylindrical Equal Distance) global array of points. The spatial resolution of the products is 0.25°x0.25°.

3.1 *Model and assimilation*

The land surface parameterization used with the Community Climate Model (CCM3) and the Climate System Model (CSM1), the NCAR LSM has been modified as part of the development of the next version of these climate models (Bonan et al. 2001). This new model is known as the Community Land Model (CLM2). The TRMM monthly precipitation observations will be used as the precipitation input to test the model in 0.5° or higher resolution Global grid. The precipitation data processing using TMI, SSM/I and CLM model is shown in figure 1 and an example of CLM2 rain (1979-1983) shown in figure 2. Previous study (Bonan et al 2001) shows that precipitation is slightly under-estimated in winter and autumn, but the overall the model reasonably produces the annual cycle, especially the summer precipitation. Globally, the model simulates precipitation over land, which agrees with the observations. Annual precipitation is particularly well simulated for certain river basins such as Mississippi basin, Amazon River. Precipitation is over estimated by more than 45% for Congo, Yukon basins. However, model accurately, reproduces the annual precipitation. The case studies are always required for improvements in the model performance; we are in the preliminary stage of incorporating into CLM precipitation.

We have tested the GLDAS approach for total precipitation estimation using SSM/I and TMI microwave data. GLDAS is an offline land model driven by

atmospheric observations and analysis data. GLDAS is a 0.25° and higher resolution near-real time. GLDAS is a combined effort led by researchers at NASA's Goddard Space Flight Center and NOAA's National Centers for Environmental Prediction (NCEP), in collaboration with researchers at Princeton, the University of Washington and the National Weather Service (NWS) office of Hydrology (Houser et al. 2000, Rodell et al. 2002) The uncertainties of the atmospheric parameters will be minimized using GLDAS. The model assumptions and initial land conditions for modeling and data assimilation is provided by GLDAS. Improvements in assimilating TMI and SSM/I rain rate to improve hydrological cycle and climate parameters are key scientific research objectives. The 3-hour rain rate derived from TMI, SSM/I and other data shows improvement in global precipitation analysis. TMI, SSM/I rain data gives much better results as compared to Geostationary Infrared data. The results provided and illustrated in this paper shows that the precipitation assimilation using microwave data can improve the climate and other application significantly. Higgins rain gauge daily accumulated data (0.25° x 0.25° grid) and NEXt generation RADar (NEXRAD) stage IV hourly radar data for continental U.S. is used in this study. Precipitation derived from Geostationary IR, Microwave data is compared with Higgins gauge data and stage IV NEXRAD data from NOAA.

4. TRMM AND OTHER DATA RAIN ESTIMATE

Near-real time satellite-derived precipitation data sets are derived from NASA/GSFC (Huffman 2001) and the U.S. Naval Research Laboratory (NRL). The NRL produces precipitation based on both geostationary satellite infrared cloud top temperature measurements and microwave observation techniques (Turk et al. 2000). These precipitation datasets have a spatial resolution of 0.25° x 0.25° and a temporal resolution of 3 hours with 60° S to 60° N coverage.

The system to produce the "TRMM and Other Data" estimates in real-time was developed (Huffman et al. 2002) to apply new concepts in merging quasi-global precipitation estimates and to take advantage of the increasing availability of input data sets in near real time. The product is produced quasi-operationally on a best-effort basis at TSDIS, with on-going scientific development by a research team in the GSFC Laboratory for Atmospheres. There are three "TRMM and Other Data" products (Huffman et al. 2002):

4.1 *3B40RT (High Quality, or HQ)*

This data product merges all available SSM/I and TMI microwave precipitation estimates into a "high-quality" (HQ) precipitation estimate. The SSM/I estimates are computed with the GPROF 5.0-SSMI algorithm and the TMI estimates are computed with the GPROF 5.0-TMI algorithm (the real-time TRMM 2A12 product). Before merger the SSM/I are calibrated to the TMI using separate global land and ocean matched histograms (Huffman et all 2002). All the fields are on a 0.25° x 0.25° grid. Grid box edges are on multiples of 0.25°. All fields are 1440x720 grid boxes (0-360° E, 90° N-S). The first grid box center is at (0.125° E, 89.875° N). Files are produced every 3 hours on synoptic observation hours (00 UTC, 03 UTC, ..., 21 UTC) as an accumulation of all HQ swath data observed within +/-90 minutes of the nominal file time. Estimates are only computed for the band 70° N-S. Figure 3 shows the precipitation estimation at 12 Z on February 4, 2002.

4.2 *3B41RT (Variable Rain rate Infrared, or VAR)*

This is the precipitation estimate from geostationary infrared (IR) observations using spatially and temporally varying calibration by the HQ. The algorithm is a probability-matched threshold approach that ensures that the histogram of grid box-average IR precipitation rates matches the histogram of grid box-average HQ precipitation rates locally (Huffman et al. 2002). As such, the colder an IR pixel is than the zero-precipitation threshold brightness temperature, the higher the rain rate it receives. It was referred as the variable-rain rate (VAR) infrared algorithm. All fields are 1440x480 grid boxes (0-360° E, 60° N-S). The first grid box center is at (0.125° E, 59.875° N). Files are produced every hour from the on-hour IR image (except for the half-past image for GMS), with fill-in by the half-past image (except for GMS, where the on-hour image is used for fill-in). Valid estimates are only provided in the band 50° N-S. Figure 4 shows the infrared precipitation estimate on February 4, 2002 at 12 Z.

4.3 *3B42RT (Merger of HQ and VAR)*

It is a merger of 3B40RT (HQ) and 3B41RT (VAR). The current scheme is simple replacement for each grid box the HQ value is used if available, and otherwise the VAR value is used (Huffman et al. 2002). All fields are 1440x480 grid boxes (0-360° E, 60° N-S). The first grid box center is at (0.125° E, 59.875° N). Files are produced every 3 hours on synoptic observation hours (00 UTC, 03 UTC, ..., 21 UTC) using that hour's 3B40RT and 3B41RT data sets. Valid estimates are only provided in the band 50° N-S. Both precipitation and random error are scaled by 100 before conversion to 2-byte integer. Thus, units are 0.01 mm/h. To recover the original floating-point values in mm/h, divide by 100. Missings are given the 2-byte-integer missing value, -31999. The remaining fields are in numbers of pixels, except the source variable, which is dimensionless. The merged precipitation estimate on February 4, 2002 at 12Z is shown in Figure 5.

The validity of the ambiguous/missing pixels is difficult to determine but the validity of the rain or no rain data is examined. 3B40RT precipitation values that are highly likely to be artifacts (number of ambiguous pixels at least 40% of the total number of pixels) are encoded as (-p - 0.01), where "P" is the original precipitation value, before conversion to scaled 2-byte-integer (Huffman et al. 2002). The estimated value in grid boxes is determined and the non-negative precipitation values are checked. 3B41RT and 3B42RT precipitation values outside the 50° N-S latitude band are considered experimental and are encoded as (-p 0.01), where "P" is the original precipitation value, before conversion to scaled 2-byte-integer (Huffman et al 2002). The 3B42RT "source of estimate" field only has three discrete values, 1, 0, 100, which correspond to "no estimate", "HQ", and "VAR".

Despite a number of areas in which precipitation estimation improvements are being sought and there are numerous similar data sets. There are several errors and difficulties in the rain accuracy estimation, which can be fixed. All the attributes of being fine-scaled in space and time, quasi-global, near-real-time, inter-calibrated, and formed by combining multiple data sources. The closest is the set of estimates based on Turk (1999), which uses individual SSM/I overpasses to calibrate geo-IR precipitation estimates. Several SSM/I-based data sets are available as gridded single-sensor data sets with significant data voids in cold-land, snow-covered, and ice-covered areas, including those computed with the GPROF 6.0 algorithm (based on Kummerow et al. 1996) and the NOAA Scattering algorithm (Grody 1991), among others. Other daily, single-sensor data sets are available for open-water regions based on SSM/I data (Wentz and Spencer 1998) or MSU data (Spencer 1993). Numerous daily single-sensor or combination data sets are available at the regional scale, but are not really "similar."

5. DATA ANALYSIS AND ERROR DETECTION

Validation and inter-comparison study is performed using satellite products and Higgins rain gauge and NEXRAD radar data. We compare the difference between satellite derived global precipitation such as Geostationary IR total precipitation in mm for October 9, 2002 (Shown in figure 6), TMI and SSM/I total precipitation (figure 7), NASA Merged total precipitation (figure 8) with GLDAS model derived total precipitation (figure 9). We found over all good agreement among microwave total precipitation products. Geostatinary IR total precipitation is also agreed well with microwave total precipitation data except some spots.

Another set of precipitation data product not global but on US continental scale are compared and validated which are illustrated in figure 10 to 15. Figure 10 shows the Geostationary IR total precipitation for November 1, 2002 in mm; TMI and SSM/I total precipitation is shown in figure 11; NASA merged total precipitation is shown in figure 12; and GLDAS total precipitation is shown in Figure 13. The ground validation product such Higgins gauge total precipitation and stage IV radar total precipitation is shown in figure 14 and 15 respectively. One can confer from these images that the microwave products such as TMI and SSM/I total precipitation agree well with NASA merged total precipitation and also with ground validation data such as Higgins total precipitation and NEXRAD radar total precipitation. The performance of GLDAS model total precipitation is reasonably well as compared to microwave product and ground validation total precipitation. The performance of the Geostationary IR total precipitation product is not that good as compared to microwave data products and ground validation datasets, one can conclude that there is precipitation over estimation in North-western region of United States.

Several types of known errors in the precipitation dataset especially in the SSM/I datasets are detected. Built-in hot- and cold-load calibration checks are used to convert counts to Antenna Temperature (T_a). An algorithm has been developed to convert T_a to Brightness Temperature (T_b) for the several different channels eliminating cross-channel leakage. The systematic navigation corrections are applied. All pixels with non-physical T_b and local calibration errors are deleted. Accuracies in the T_b's are within the uncertainties of the precipitation estimation techniques. For the most part, tests show only small differences among the SSM/I sensors flying on different platforms. The SSM/I scattering field is probably not reliable and must be small in snow filled land areas. Some satellites experienced significant drifting of the equator-crossing time during their period of service. There is no direct effect on the accuracy of the SSM/I data, but it is possible that the systematic change in sampling time could introduce biases in the resulting SSM/I-only precipitation estimates (Huffman et al. 2002).

Because of the similarity in frequencies, TMI error detection/correction is quite similar to that of the SSM/I. The TMI is a modified SSM/I with the 10 GHz channels added. Built-in hot- and cold-load calibration checks are used to convert counts to Antenna Temperature (T_a). An algorithm converts T_a to Brightness Temperature (T_b) for the various channels eliminating cross-channel leakage. The systematic navigation corrections are applied to remove the sampling error. All pixels with non-physical T_b and local

calibration errors are deleted. Accuracies in the T_b's are within the uncertainties of the precipitation estimation techniques. For the most part, tests show stable cross-calibration with the fleet of SSM/I's. The GROF has strong correlation coefficient with gauge data, which is above 0.77 (Huffman et al 2002). There is no direct effect on the accuracy of the TMI data, but the continually changing diurnal sampling can cause significant fluctuations in the resulting TMI-only precipitation estimates (Huffman et al. 2002). The observations uniformity on pixel to pixel basis and warm bias correction of the TMI can provide precise radiometric calibration.

6. DISCUSSION AND CONCLUSION

The results presented in this research shows that the microwave rain estimation is much superior that the infrared estimation. The microwave total precipitation estimation agrees well with each other and also with the ground validation datasets including NEXRAD total precipitation. Good agreements are found in microwave total precipitation and the GLDAS model total precipitation. The performance of the model in total precipitation estimation and assimilation is reasonably good.

Improvements have been made in TRMM passive microwave rain estimation. The accuracy of the precipitation products can be subdivided into systematic departures from the true answer (bias) and random fluctuations about the true answer (sampling), as discussed in Huffman (1997). The former are the biggest problem for climatological averages, since they will not average out. However, for short averaging periods the low number of samples and/or inaccuracies in algorithm can provide a more serious problem for SSM/I and TMI. The distribution of precipitation over the day as sampled may not be the true precipitation value. For VAR, the sampling is good, but the algorithm likely has substantial RMS error due to the weak physical connection between IR T_b's and precipitation. Accordingly, the "random error" is assumed to be dominant, and estimates could be computed as discussed in Huffman (1997). Random error cannot be corrected. The "bias error" is likely small, or at least contained. This is less true over land, where the lower-frequency microwave channels are not useful for precipitation estimation with our current state of knowledge. Studies of the sub-monthly bias have not yet been performed. The cause of shift in orbit can contribute significant amount of error and can grow by time say days, weeks. The over flight times to the nearest minute is generally reliable. The error sources can be also minimized by assessing how accurate one can estimate the start time and position of each orbit. The Real Time data set inter-comparison results are still being developed. The time series of the global images shows good continuity in time and space across the geo-IR data boundaries.

Several precipitation measurements are in different scales and formats, different variability and the different uncertainties depending on sensor techniques which makes difficult to get precipitation in desired scale and time. Precipitation and the associated latent heating play important roles in controlling the Earth's general circulation, which leads to the variations in weather systems and climate processes. In addition, atmospheric processes are intricately linked to hydrologic, oceanic, and land surface processes through precipitation fluxes. GLDAS project and other agencies seek to determine the Earth system's variability, forcing, responses, change consequences, and likelihood of predictability. The measurement of precipitation at temporal and spatial scales concomitant with the actual scales of rain production, sorting, distribution, and fallout becomes essential.

Acknowledgement

The Real Time (RT) Data Set were provided by the NASA/Goddard Space Flight Center's Laboratory for Atmospheres and TSDIS, which develop and compute the RT Data Set as a contribution to TRMM. This research was supported by National Research Council's postdoctoral research associateship award. We would like to thank Dr. George Huffman for his help and discussion during this investigation and Dr. Erich Schocker, TSDIS, for providing TRMM data and software support. GLDAS supports provided by Brian Cosgrove and Jon Gottschalck are acknowledged.

References

Adler, R.F., G.J. Huffman, D.T. Bolvin, S. Curtis, and E.J. Nelkin, 2000: Tropical rainfall distribution determined using TRMM combined with other satellite and rain gauge information. Journal of Applied Meteorology, **39**, 2007-2023.

Ba, M.B., and A. Gruber, 2001: GOES multispectral rainfall algorithm (GMSRA). Journal of Applied Meteorology, **40**, 1500-1514.

Bonan, G. B., K.W. Oleson, M. Vertenstein, S. Levis, X. Zeng, Y. Dai, E. Dickinson and Z. Yang, 2001: The Land Surface Climatology of the Community Land Model Coupled to the NCAR Community Climate Model, Submitted to Journal of Climate, December 2001.

Bellerby, T., M. Todd, D. Kniveton, and C. Kidd, 2000: Rainfall estimation from a combination of TRMM precipitation radar and GOES multispectral satellite

imagery through the use of an artificial neural network. Journal of Applied Meteorology, **39**, 2115-2128.

Grody, N.C., 1991: Classification of snow cover and precipitation using the Special Sensor Microwave/Imager (SSM/I). Journal Geophysical Research, **96**, 7423-7435.

Hollinger, J.P., J.L. Pierce, and G.A. Poe, 1990: SSM/I instrument evaluation. IEEE Transactions on Geoscience and Remote Sensing, **28**, 781-790.

Houser P. R., Bosilovich M., Cosgrove B., Entin J. K., Wlaker J., Pan H.-L., Mitchell K., (2000): A Global Land Data Assimilation Scheme (GLDAS), research proposal submitted to NASA-ESE (ldas.gsfc.nasa.gov).

Huffman, G.J., 1997: Estimates of root-mean-square random error contained in finite sets of estimated precipitation. Journal of Applied Meteorology, **36**, 1191-1201.

Huffman G.J., R.F. Adler, E.F. Stocker, D.T. Bolvin, E.J. Nelkin (2002): A TRMM-based Quasi-Global merged precipitation estimates. NASA TRMM conference, Honolulu, Hawaii, July 22-26, pp 7 (NASA/TM-2002-211605)

Janowiak, J.E., and P.A. Arkin, 1991: Rainfall variations in the tropics during 1986-1989. Journal of Geophysical Research, **96**, 3359-3373.

Joyce, R.J., J.E. Janowiak, G.J. Huffman, 2001: Latitudinal and Seasonal Dependent Zenith Angle Corrections for Geostationary Satellite IR Brightness Temperatures. Journal of Applied Meteorology, **40(4)**, 689-703.

Kummerow, C., W.S. Olsen, and L. Giglio, 1996: A simplified scheme for obtaining precipitation and vertical hydrometeor profiles from passive microwave sensors. IEEE Transactions on Geoscience and Remote Sensing, **34**, 1213-1232.

Kummerow, C, J. Simpson, O. Thiele, W. Barnes, A.T.C. Chang, E. Stocker, R.F. Adler, A. Hou, R. Kakar, F. Wentz, P. Ashcroft, T. Kozu, Y. Hong, K. Okamoto, T. Iguchi, H. Kuroiwa, E. Im, Z. Haddad, G. Huffman, B. Ferrier, W.S. Olson, E. Zipser, E.A. Smith, T.T. Wilheit, G. North, T. Krishnamurti, and K. Nakamura, 2000: The status of the Tropical Rainfall Measuring Mission (TRMM) after two years in orbit. Journal Applied Meteorology, **39**, 1965-1982.

Kummerow, C., W. Barnes, T. Kozu, J. Shiue, and J. Simpson, 1998: The Tropical Rainfall Measuring Mission (TRMM) Sensor Package. Journal of Atmospheric and Oceanic Technology, **15(3**), 809-817.

Li, Q., R.L. Bras, and D. Veneziano, 1996: Analysis of Darwin rainfall data: Implications on sampling strategy. Journal of Applied Meteorology, **35**, 372-385.

Morrissey, M.L., and J.E. Janowiak, 1996: Sampling-induced conditional biases in satellite climate-scale rainfall estimates. Journal of Applied Meteorology, **35**, 541-548.

Nirala M. L. and A.P. Cracknell, 2002a: Microwave measurement of rain and sea surface temperature from the TMI., International Journal of Remote Sensing, **23**, No. 13,2673-2691.

Nirala M. L. and A. P. Cracknell, 2002b: Estimation of three-dimensional distribution of rain from precipitation radar over Indian region, International Journal of Remote Sensing, (in press).

Olson, W. S., C. D. Kummerow, Y. Hong, and W.-K. Tao, 1999: Atmospheric latent heating distributions in the tropics derived from satellite passive microwave radiometer measurements. Journal of Applied Meteorology, **38**, 633-664.

Rodell, M.,P.R. Houser, U. Jambor, J. Gottschalck, C-J. Meng, K. Arsenault, B. Cosgrove, J. Radakovich, M. Bosilovich, J. K. Entin, J. K. Walker, and K. Mitchell, 2002: The Global Land Data Assimilation System (GLDAS), Submitted to Bulletin of American Meteorological Society.

Simpson, J., C. Kummerow, W.-K. Tao, and R.F. Adler, 1996: On the Tropical Rainfall Measuring Mission (TRMM) satellite. Meteorology and Atmospheric Physics, **60**, 19-36.

Smith, E.A., C. Kummerow, and A. Mugnai, 1994: The emergence of inversion-type precipitation profile algorithms for estimation of precipitation from satellite microwave measurements. Remote Sensing Reviews, **11**, 211-242.

Smith, E.A., J. Lamm, R. Adler, J. Alishouse, K. Aonashi, E. Barrett, P. Bauer, W. Berg, A. Chang, R. Ferraro, J. Ferriday, S. Goodman, N. Grody, C. Kidd, D. Kniveton, C. Kummerow, G. Liu, F. Marzano, A. Mugnai, W. Olson, G. Petty, A. Shibata, R. Spencer, F. Wentz, T. Wilheit, and E. Zipser, 1998: Results of WetNet PIP-2 project. Journal of Atmospheric Science, **55**, 1483-1536.

Soman, V.V., J.B. Valdes, and G. North, 1995: Satellite sampling and the diurnal cycle statistics of Darwin rainfall data. Journal of Applied Meteorology, **34**, 2481-2490.

Spencer, R.W., 1993: Global oceanic precipitation from the MSU during 1979-92 and comparisons to other climatologies. Journal of Climate, **6**, 1301-1326.

Shepherd J.M., E. A. Smith and W.J. Adams, (2002): Global precipitation measurement-Report 7: Bridging from TRMM to GPM to 3-hourly precipitation estimates. NASA/TM-2002-211602, April 2002.

Turk, F.J., G.D. Rohaly, J. Hawkins, E.A. Smith, F.S. Marzano, A. Mugnai, and V. Levizzani, 1999: Meteorological applications of precipitation estimation from combined SSM/I, TRMM and infrared geostationary satellite data. Microwave Radiometry and Remote Sensing of the Earth's Surface and Atmosphere, P. Pampaloni and S. Paloscia Eds., VSP International Science Publication, 353-363.

Turk, F. J., G. Rohaly, J.D. Hawkins, E.A. Smith, A. Grose, F.S. Marzano, A. Mugnai and V. Levizzani, 2000: Analysis and assimilation of rainfall from blended SSM/I, TRMM and geostationary satellite data, AMS 10th conf. On Satellite Meteorology and Oceanography, Long Beach, CA, 9-14 January, 66-69.

Wentz, F.J., and R.W. Spencer, 1998: SSM/I rain retrievals within a unified all-weather ocean algorithm. Journal of Atmospheric Science, **55(9)**, 1613-1627.

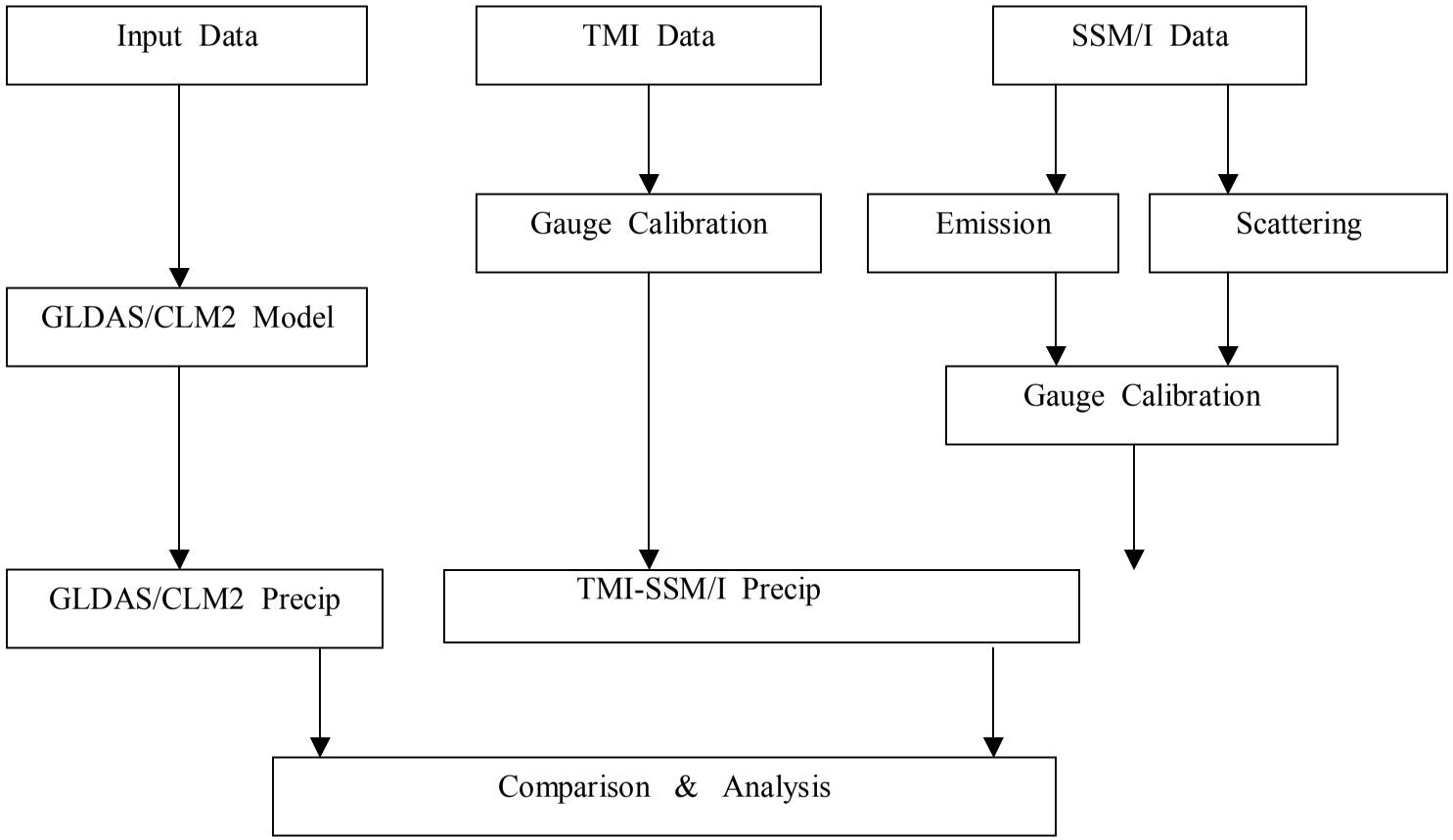

Figure 1: Precipitation data processing using TMI, SSM/I and GLDAS/CLM2 model.

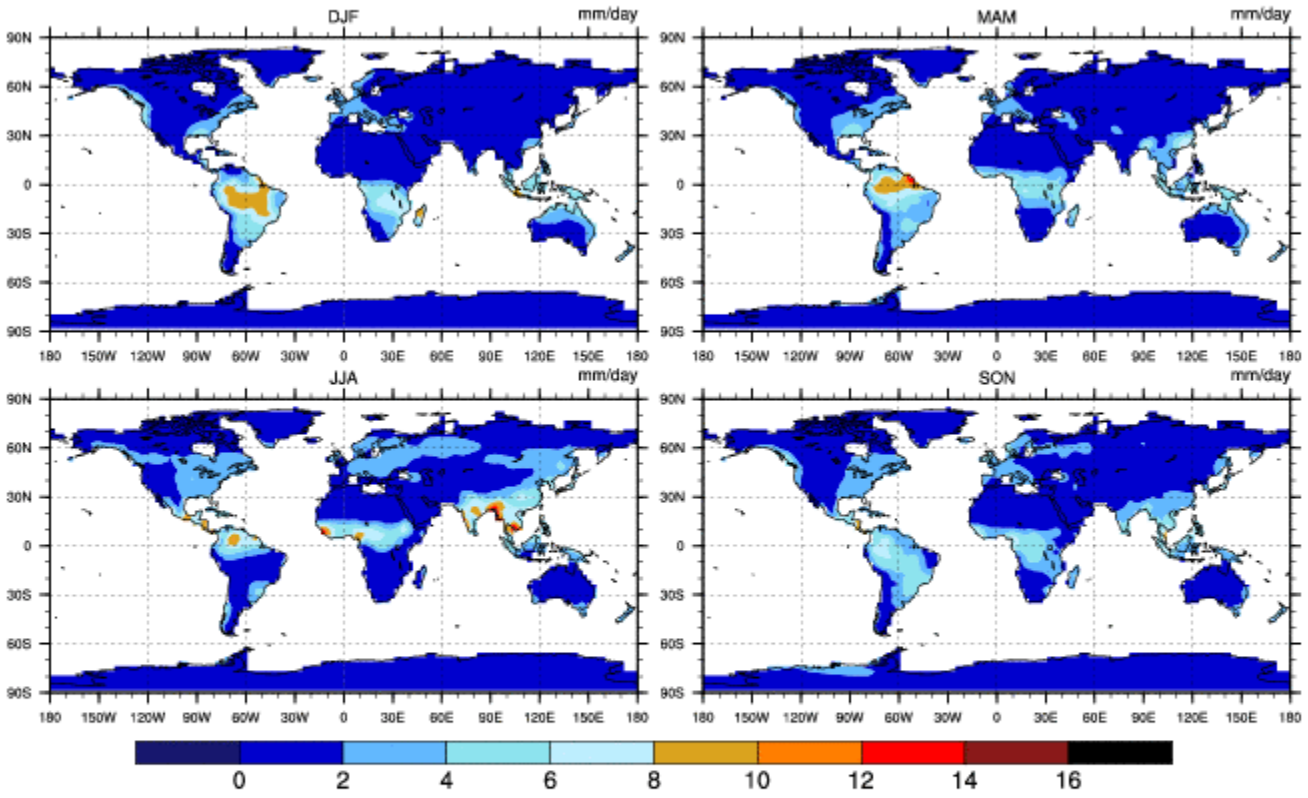
DJF
mm/day
MAM
mm/day
JJA
mm/day
SON
mm/day
90N
60N
30N
0
30S
60S
90S
180 150W 120W 90W 60W 30W 0 30E 60E 90E 120E 150E 180
0 2 4 6 8 10 12 14 16

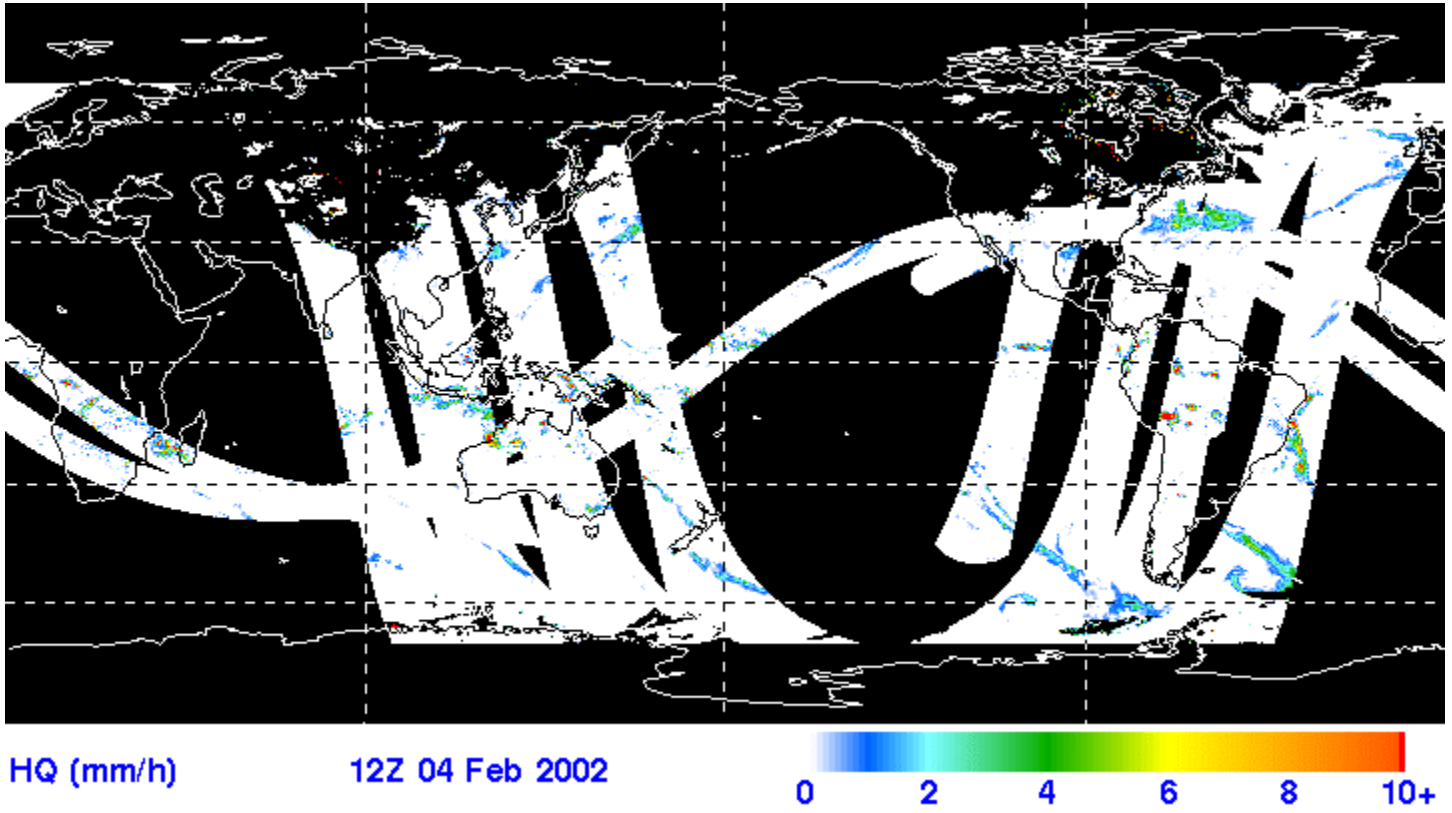

Figure 3: TMI and SSM/I merged Precipitation estimation (3B40RT) at 12 Z on February 4, 2002.

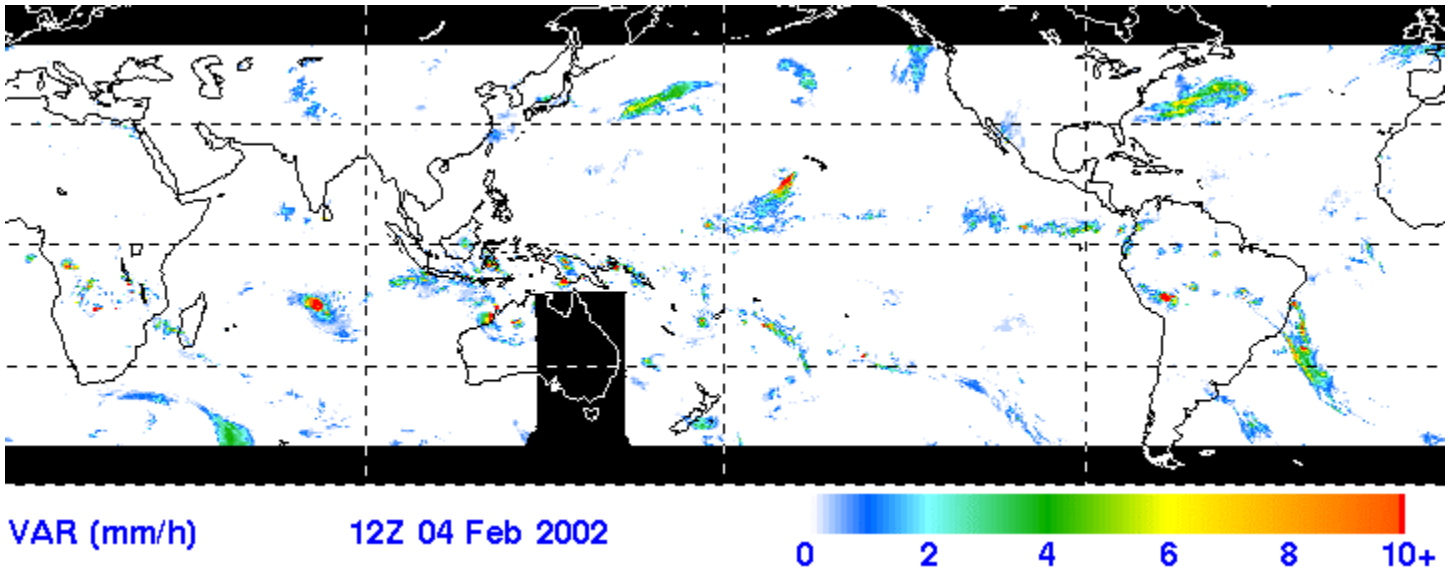

Figure 4: Geostationary IR Precipitation estimation (3B41RT) at 12 Z on February 4, 2002

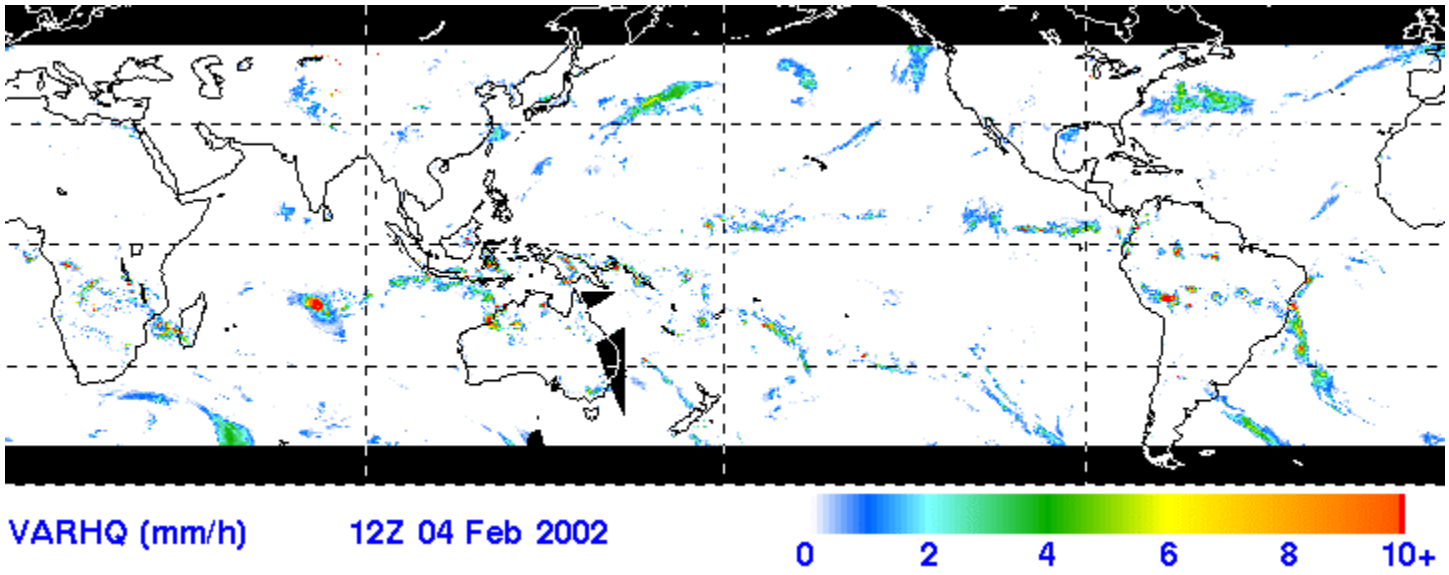

Figure 5: Merged TMI, SSM/I and Geo-IR Precipitation estimation (3B42RT) at 12 Z on February 4, 2002

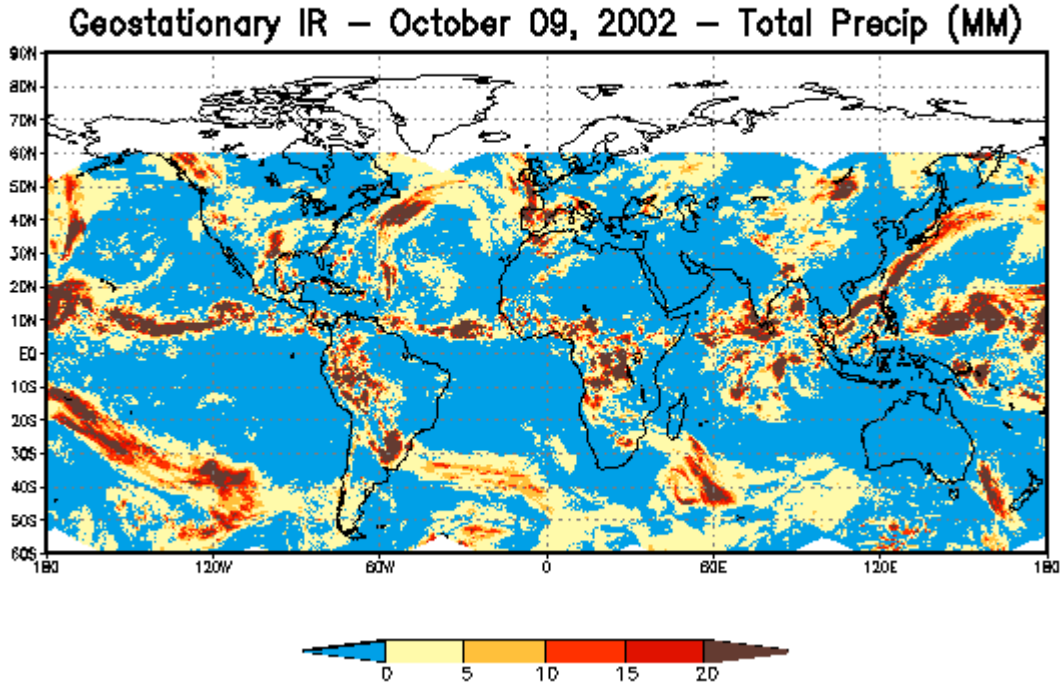

Figure 6: Total Precipitation estimation using Geostationary InfraRed Data

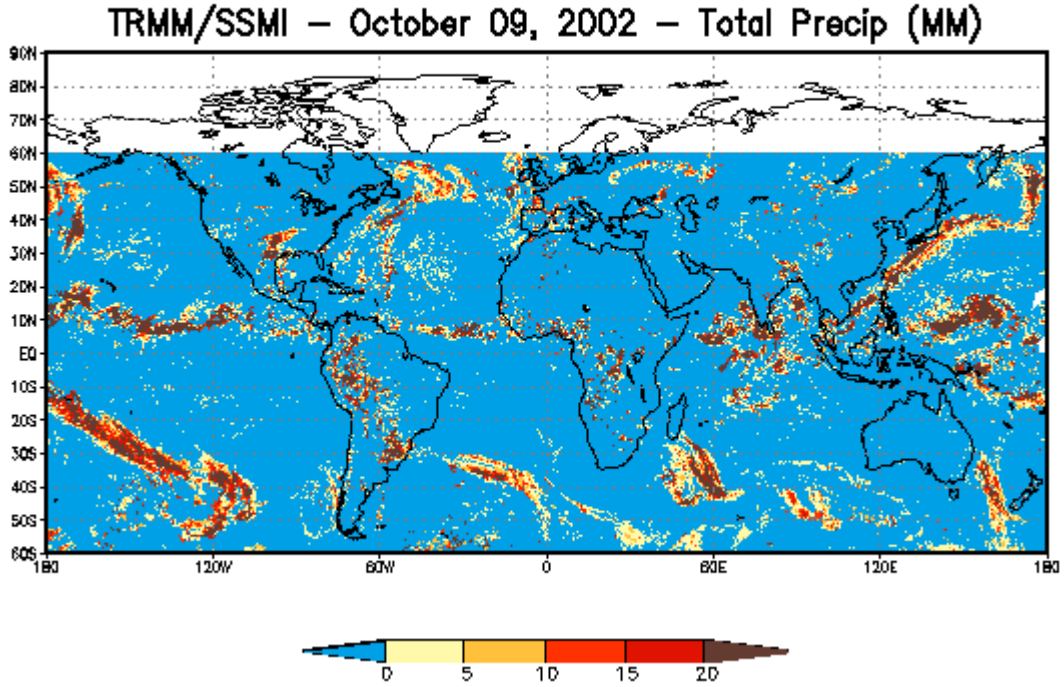

Figure 7: TRMM-TMI/DMSP-SSM/I Total Precipitation

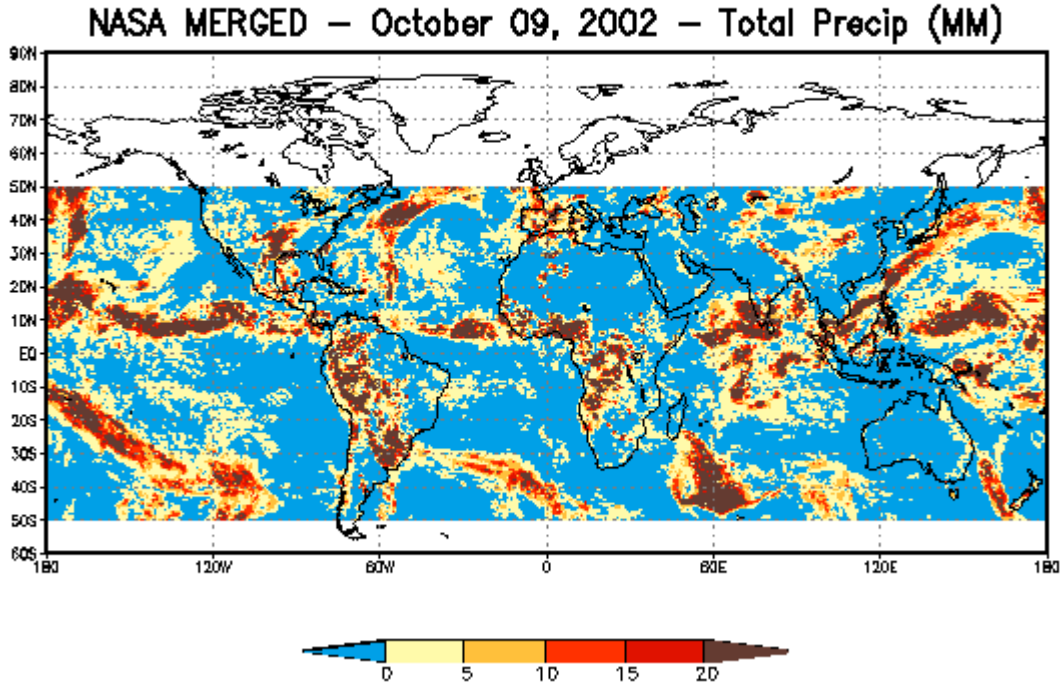

Figure 8: NASA merged (Microwave and IR) Total Precipitation

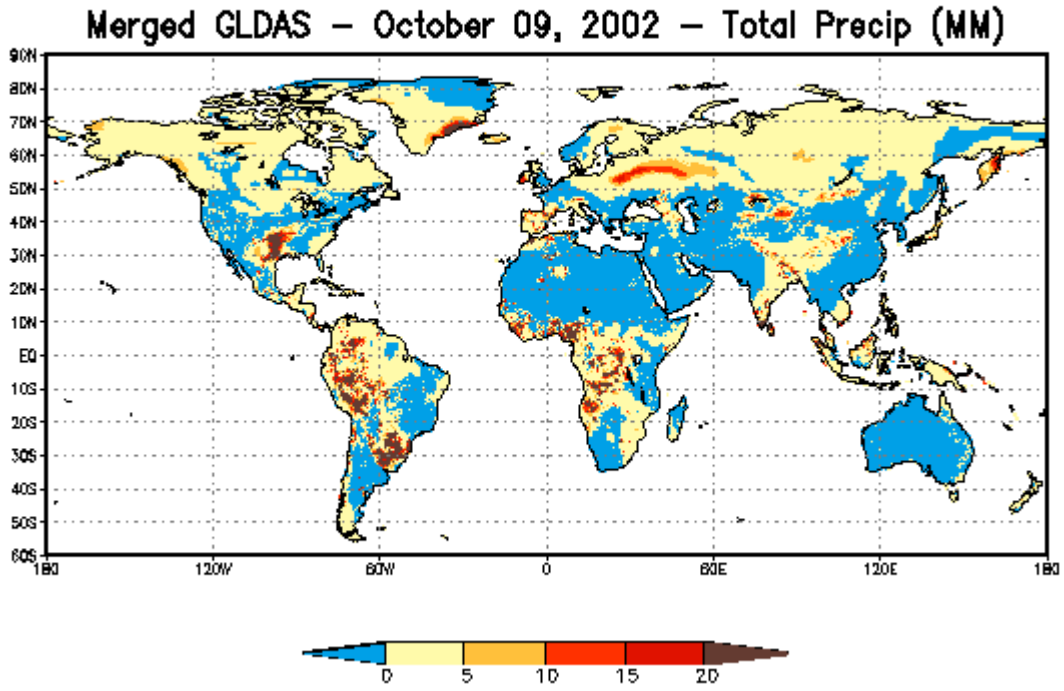

Figure 9: Merged (Microwave and Infrared) GLDAS Total Precipitation

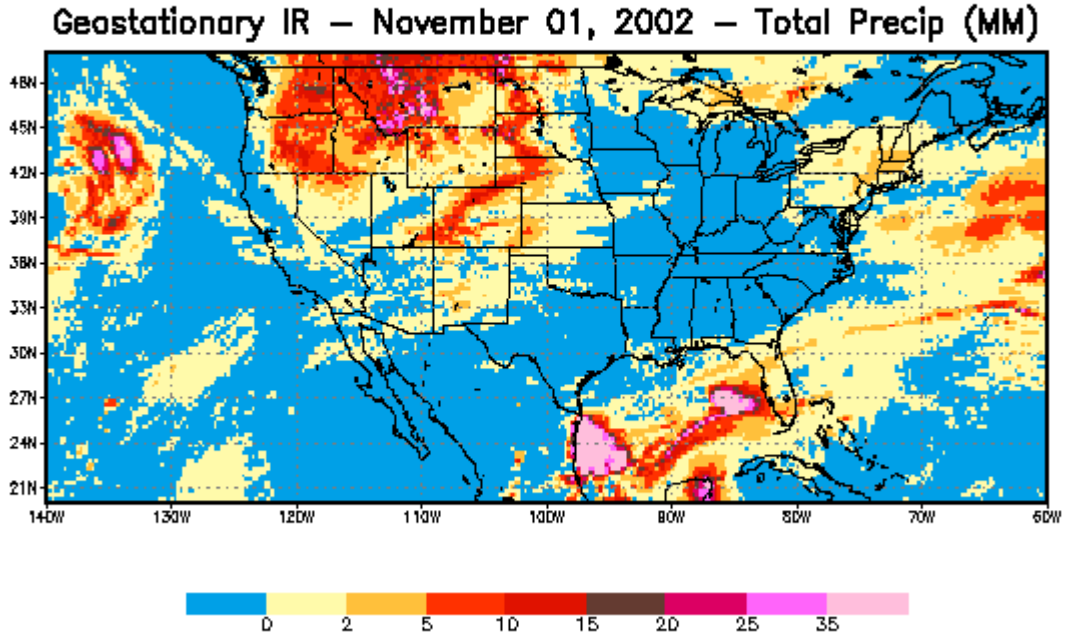

Figure 10: Geostationary InfraRed Total Precipitation

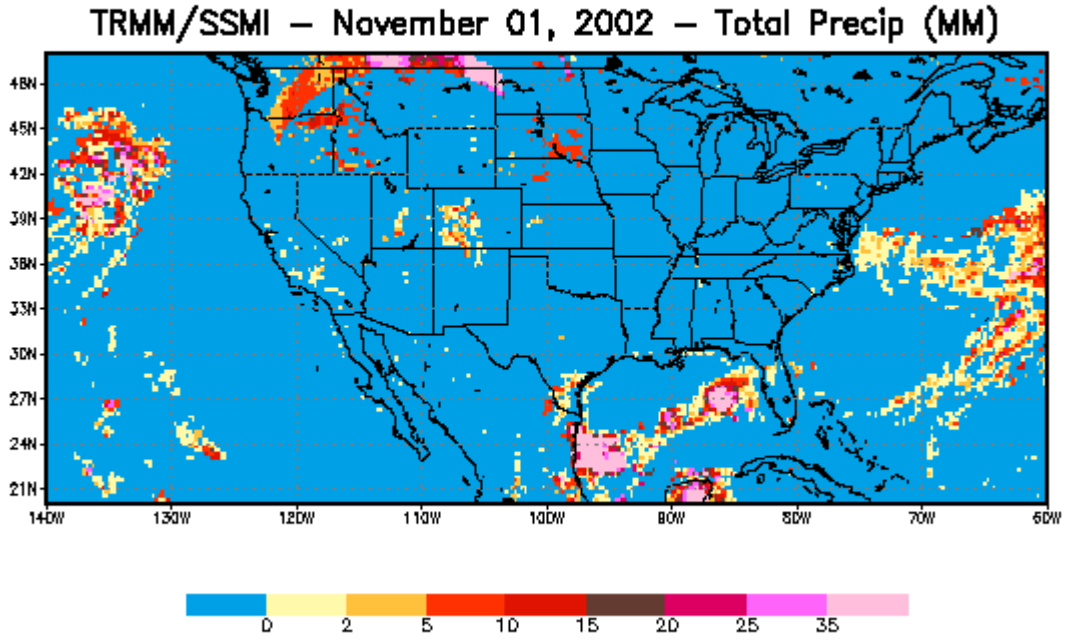

Figure 11: TRMM-TMI/DMSP-SSM/I Total Precipitation

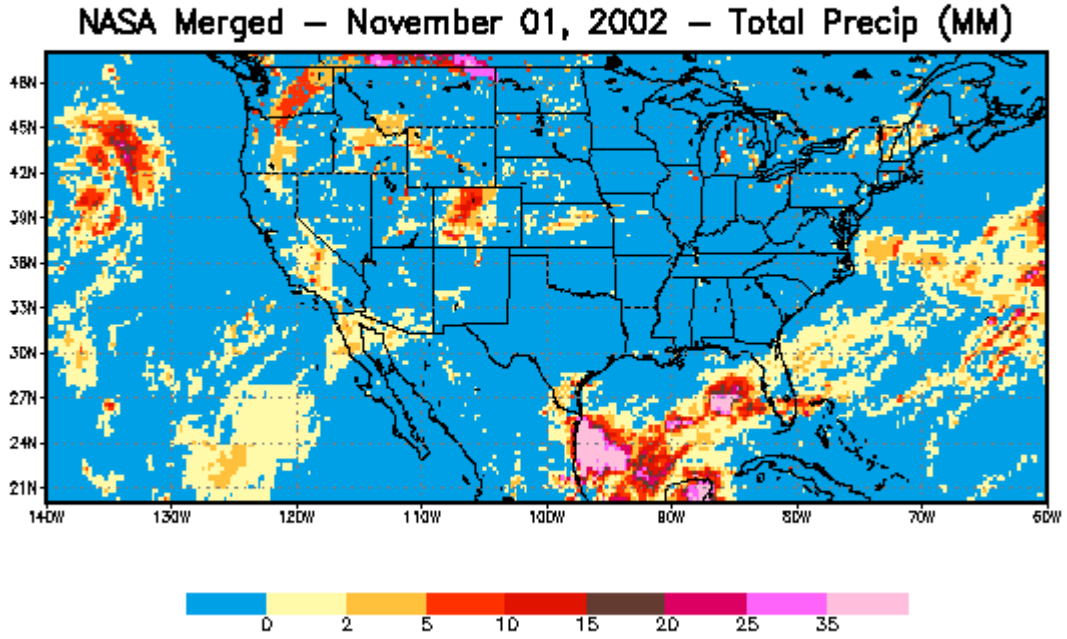

Figure 12: NASA Microwave/Infrared merged Total Precipitation

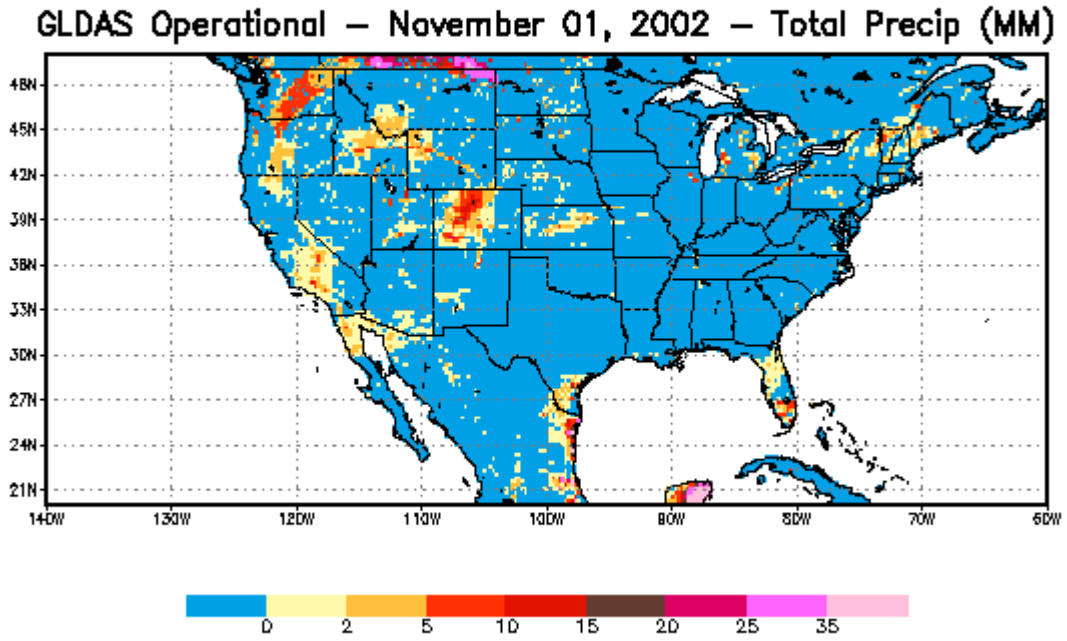

Figure 13: GLDAS Merged Total Precipitation

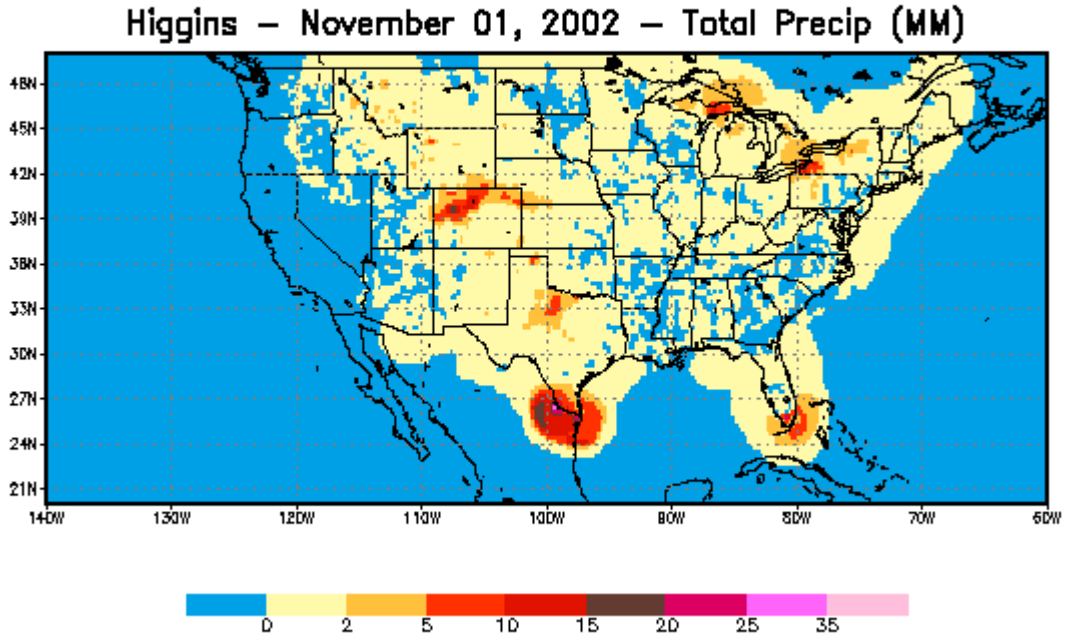

Figure 14: Higgins Rain Gauge Total Precipitation

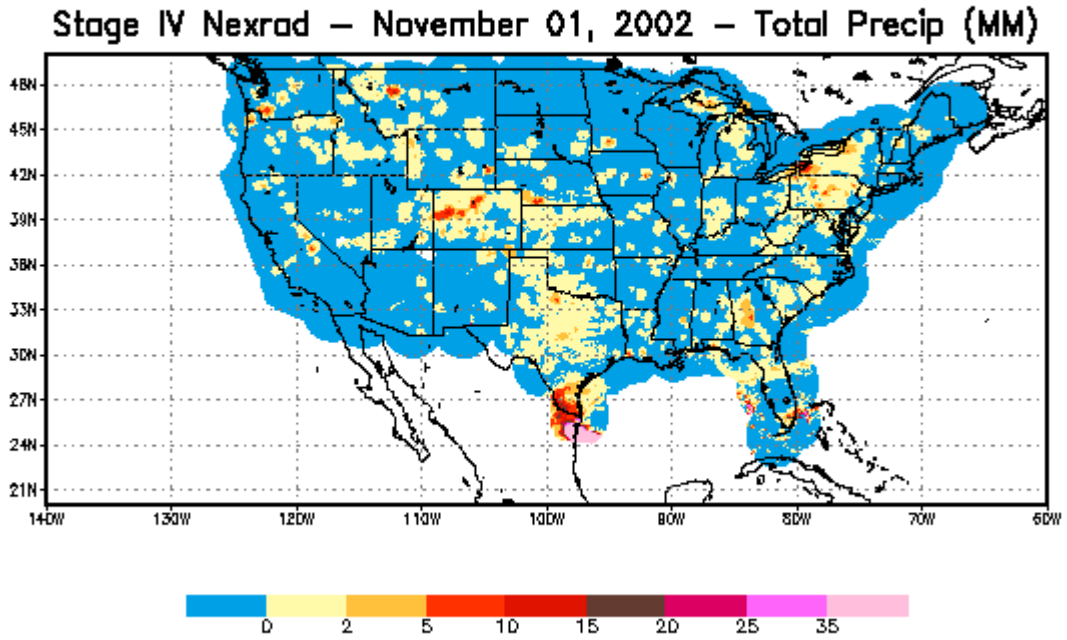

Figure 15: Nexrad Ground-based Radar Total Precipitation